2016

Evidence for differential glycosylation of trophoblast cell types

Qiushi Chen
Imperial College London

Poh-Choo Pang
Imperial College London

Marie E. Cohen
University of Geneva

Mark S. Longtime
Washington University School of Medicine

Danny J. Schust
University of Missouri

See next page for additional authors

Research

Evidence for Differential Glycosylation of Trophoblast Cell Types*[S]

Qiushi Chen‡, Poh-Choo Pang‡, Marie E. Cohen§, Mark S. Longtine¶, Danny J. Schust‖, Stuart M. Haslam‡, Sandra M. Blois**¶¶, Anne Dell‡¶¶, and Gary F. Clark‖¶¶

Human placental villi are surfaced by the syncytiotrophoblast (STB), with a layer of cytotrophoblasts (CTB) positioned just beneath the STB. STB in normal term pregnancies is exposed to maternal immune cells in the placental intervillous space. Extravillous cytotrophoblasts (EVT) invade the decidua and spiral arteries, where they act in conjunction with natural killer (NK) cells to convert the spiral arteries into flaccid conduits for maternal blood that support a 3–4 fold increase in the rate of maternal blood flow into the placental intervillous space. The functional roles of these distinct trophoblast subtypes during pregnancy suggested that they could be differentially glycosylated. Glycomic analysis of these trophoblasts has revealed the expression of elevated levels of biantennary N-glycans in STB and CTB, with the majority of them bearing a bisecting GlcNAc. N-glycans terminated with polylactosamine extensions were also detected at low levels. A subset of the N-glycans linked to these trophoblasts were sialylated, primarily with terminal NeuAcα2–3Gal sequences. EVT were decorated with the same N-glycans as STB and CTB, except in different proportions. The level of bisecting type N-glycans was reduced, but the level of N-glycans decorated with polylactosamine sequences were substantially elevated compared with the other types of trophoblasts. The level of triantennary and tetraantennary N-glycans was also elevated in EVT. The sialylated N-glycans derived from EVT were completely susceptible to an α2–3 specific neuraminidase (sialidase S). The possibility exists that the N-glycans associated with these different trophoblast subpopulations could act as functional groups. These potential relationships will be considered. ***Molecular & Cellular Proteomics 15: 10.1074/mcp.M115.055798, 1857–1866, 2016.***

Human development *in utero* requires the formation of a functional placenta that mediates the transport of nutrients, the exchange of gases, and the production of hormones that are required to maintain fetal viability. The placenta also serves as the immune interface between the mother and her histoincompatible fetus. Human trophoblasts are specialized placental cells that come into direct physical contact with maternal immune cells at both the villous surface and within the maternal decidua and myometrium. The syncytiotrophoblast (STB)[1] layer is localized to the villous surface, with subsyncytial cytotrophoblasts (CTB) lying just beneath the STB. Regions of the syncytium can become damaged, which occurs at an increased frequency in many complicated pregnancies, and this damage can be repaired by division and fusion of cytotrophoblasts. It is likely that CTB in these damaged regions are at least transiently in direct contact with circulating maternal immune cells (1, 2).

Extravillous cytotrophoblasts (EVT) derived from placental stem cells penetrate through the tips of the anchoring villi and differentiate into invasive trophoblasts that migrate into the decidua, myometrium and spiral arteries (3). Trophoblasts that enter the spiral arteries differentiate into endovascular cytotrophoblasts. These cytotrophoblasts act in concert with maternal NK cells to remodel these arteries into flaccid conduits that support a three- to fourfold increase in the rate of maternal blood flow into the placental intervillous space at a reduced pressure compared with the maternal circulation (4–6).

From the ‡Department of Life Sciences, Imperial College London, London SW7 2AZ, United Kingdom; §Department of Gynaecology and Obstetrics, Faculty of Medicine, Geneva, Switzerland; ¶Department of Obstetrics and Gynecology, Washington University, School of Medicine, St. Louis, Missouri 63110; ‖Division of Reproductive and Perinatal Research, Department of Obstetrics, Gynecology and Women's Health, School of Medicine, University of Missouri, Columbia, Missouri 65212; **Charité Center for Internal Medicine and Dermatology, Division of General Internal and Psychosomatic Medicine, Reproductive Medicine Research Group, Charité-Universitätsmedizin Berlin, Berlin, Germany

Received October 14, 2015, and in revised form, February 18, 2016
Published, MCP Papers in Press, February 29, 2016, DOI 10.1074/mcp.M115.055798

Author contributions: S.M.H., S.M.B., A.D., and G.F.C. designed research; Q.C., P.P., M.E.C., and M.S.L. performed research; Q.C., P.P., M.E.C., M.S.L., D.J.S., S.M.H., S.M.B., A.D., and G.F.C. analyzed data; Q.C., P.P., M.S.L., D.J.S., A.D., and G.F.C. wrote the paper.

[1] The abbreviations used are: STB, syncytiotrophoblast; BBSCT, biantennary bisected type; CFG, Consortium for Functional Glycomics; CTB, cytotrophoblasts; dNK, decidual natural killer; EVT, extravillous cytotrophoblasts; HLA, human leukocyte antigen; LacNAc, N-acetyllactosamine; NK, natural killer; PAEP, progestagen-associated endometrial protein; PMAA, partially methylated alditol acetate.

Interactions between villous trophoblasts and maternal immune cells would normally be expected to trigger major histocompatibility responses because of the expression of paternal human leukocyte antigens (HLA). However, STB and CTB do not express the HLA class I molecules that are necessary to evoke such responses (7, 8). This absence of HLA molecules on STB and CTB could make these trophoblasts potential targets for lysis by NK cells (9). However, STB and CTB are highly resistant to lysis by peripheral blood NK cells *in vitro* (10, 11).

Unlike CTB and STB, EVT express on their cell surface a classical paternal HLA class Ia molecule designated HLA-C (7, 8). This presentation means that EVT are semiallogeneic during natural pregnancies and are therefore potentially subject to powerful histocompatibility-based immune responses. However, the activation of such responses in a manner that harms the fetus and placenta does not typically occur during normal pregnancies. How EVT evade immune recognition in the gravid human uterus remains a major enigma. In contrast to STB or CTB, EVT are also susceptible to lysis by purified decidual NK (dNK) cells (12–14). Because EVT are the precursors of endovascular trophoblasts that remodel the spiral arteries (15), increased lysis of EVT by activated dNK cells could decrease the number of endovascular trophoblasts, thereby contributing to deficient spiral artery remodeling and inadequate circulation in the intervillous space.

Glycomic analyses of glycoproteins, whole cells, tissues, and extracellular matrices have been useful for defining potential carbohydrate functional groups and their diverse roles in many cellular processes (16–21). Glycomic analysis of STB, CTB, and EVT was performed in this study to determine if the N-glycans associated with these cells have potential functional roles.

EXPERIMENTAL PROCEDURES

Isolation of CTB and STB—The protocol for obtaining placentas used for this portion of this study was approved by the Institutional Review Board of Washington University School of Medicine. Term, singleton placentas from uncomplicated pregnancies were obtained, and CTB were isolated as described previously (22, 27). All reagents were obtained from Sigma-Aldrich (St. Louis, MO) except for DNase, which was from Roche Diagnostics (Indianapolis, IN). In brief, villous tissue was isolated and digested with dispase, trypsin, and DNase and CTB were isolated on a continuous gradient of Percoll. Over 85% of the cells stained positive for cytokeratin 7, a TB specific marker. CTB were obtained after 24 h of culture in DMEM/10% FBS in 5% CO_2/air. To obtain STB, culture was continued for an additional 48 h with daily changes of medium. During this time, spontaneous differentiation and fusion occurs, with over 70% of the nuclei being present in multinucleated syncytia after 72 h of culture (22). We observed an ~50-fold increase of hCG expression from 24 to 72 h of culture, confirming efficient differentiation.

Isolation of EVT—All human tissue collection necessary for this study was approved by the local ethics committee of the Geneva University Hospital. All patients provided their informed written consent prior to their inclusion in the study. Placental tissue was obtained from patients undergoing an elective termination of pregnancy during the first trimester (8–12 weeks of gestation). The procedure for the isolation of EVT was performed as previously described (23). Placental tissue specimens were isolated and washed several times in sterile Hanks balanced salt solution. The tissue samples were subjected to enzymatic digestion five times for 20 min at 37 °C (0.25% trypsin, 0.25 mg/ml Dnase I; Roche, Diagnostics GmbH). After this incubation, fetal bovine serum (FBS) was added to neutralize the trypsin mixture. The cells were suspended in Dulbecco's modified Eagle's medium (DMEM) (Invitrogen, Switzerland). This cell suspension was filtered through a 50-μm mesh and the resulting supernatant was applied onto tubes containing a Percoll gradient (70–5% Percoll diluted with HBSS). The samples were centrifuged for 25 min at 1200 $\times$ *g*. The 30–45% Percoll layer was collected, and the trophoblast cells were harvested, washed, and resuspended in DMEM containing 10% fetal bovine serum.

The cells were transferred to Petri dishes and incubated for 15 min at 37 °C. Trophoblasts in the culture supernatants were collected by centrifugation and resuspended in culture medium. They were transferred to six-well plates (4×10^6 cells/well) and in 96-well plates (1×10^5 cells/well). After 48 h of culture, 95% of the cells were: (1) negative for vimentin; and (2) positive for cytokeratin 7 and HLA-G.

Processing of Trophoblasts to Acquire N- and O-glycans—All cell samples were subjected to a standard protocol (24). Briefly, cells were suspended in lysis buffer (25 mM Tris, 150 mM NaCl, 5 mM EDTA and 1% CHAPS (v/v), pH 7.4) before homogenization and sonication were performed. The homogenates were subsequently dialyzed against a 50 mM ammonia bicarbonate buffer, pH 7.5, after which the samples were lyophilized. Cell/tissue extracts were reduced and carboxymethylated and then treated with trypsin. The treated samples were purified using a C18 cartridge (Oasis HLB Plus, Waters, Milford, MA) prior to the release of N-glycans by peptide N-glycosidase F (recombinant from *Escherichia coli*, Roche Applied Science, Penzberg, Germany) digestion. Released N-glycans were permethylated and then purified using a Sep-Pak C18 cartridge (Waters) prior to MS analysis.

Purified, underivatized N-glycans were incubated with sialidase S (recombinant from *Streptococcus pneumonia*, Prozyme Glyko, Hayward, CA) or β1,4-galactosyltransferase (from bovine milk, Merck, Kenilworth, NJ) separately. Sialidase S digestion was carried out using sialidase S in 50 mM sodium acetate, pH 5.5. The β1,4-galactosyltransferase reaction was performed using β1,4-galactosyltransferase in 50 mM 3-(N-morpholino)-propanesulfonic acid (MOPS) containing 45 μM UDP-Gal, pH 7.4. The resulting enzyme-treated samples were lyophilized and permethylated prior to MS analysis.

Mass Spectrometric Analysis—MS data were obtained by using a Voyager-DE™ STR MALDI-TOF (Applied Biosystems, Foster City, CA) mass spectrometer. Purified permethylated glycans were dissolved in 10 μl methanol and 1 μl of the sample was mixed with 1 μl of matrix, 20 mg/ml 2,5-dihydroxybenzoic acid (DHB) in 70% (v/v) aqueous methanol and loaded on to a metal target plate. The instrument was run in the reflectron positive ion mode. The accelerating voltage was 20 kV. MS/MS data were acquired using a 4800 MALDI-TOF/TOF mass spectrometer (AB SCIEX, Framingham, MA). In the MS/MS experiment, the dissolved sample was dried and then redissolved in 10 μl methanol. 1 μl of the sample was mixed with 1 μl of matrix, 10 mg/ml diaminobenzophenone (DABP) in 70% (v/v) aqueous acetonitrile and loaded on to a metal target plate. The instrument was run in the reflectron positive ion mode. The collision energy was set to 1 kV with argon as the collision gas. The 4700 calibration standard (mass standards kit for the 4700 proteomics analyzer, Applied Biosystems) was used as the external calibrant for the MS and MS/MS modes.

GC/MS Linkage Analysis—GC-MS linkage analysis of partially methylated alditol acetates (PMAAs) was carried out using a Perkin-Elmer Life Sciences Clarus 500 instrument (Framingham, MA) fitted with

RTX-5MS column (30 m × 0.32 mm internal diameter, Restek Corp., Bellefonte, PA). The PMAAs were prepared from permethylated N-glycans as described previously (25). The permethylated glycans were hydrolyzed with 2 M trifluoroacetic acid at 121 °C for 2 h, and then reduced with 10 mg/ml sodium borodeuteride in 2 M aqueous ammonium hydroxide at room temperature for 2 h, and acetylated with acetic anhydride at 100 °C for 1 h. The sample was dissolved in hexanes and injected onto the column after the oven temperature reached 60 °C. The column was maintained at this temperature for 1 min and then heated to 300 °C at a rate of 8 °C/min. Running a blank was required before every sample analysis.

Experimental Design—

CTB N-glycans—(1) All N-glycans were presumed to have a Manα1–6(Manα1–3)Manβ1–4GlcNAcβ1–4GlcNAc core structure based on knowledge of the N-glycan biosynthetic pathway and PNGase F specificity. (2) The composition (numbers of Hex, Fuc, etc.) of the glycans derived from MALDI-TOF MS in positive ion mode were manually interpreted. (3) MALDI-TOF/TOF MS/MS analyses were carried out on the following ions: *m/z* 2592, 2635, 2837, 2850, 3141, 3212, 3300, and 3416. All MS/MS spectra were annotated manually with the assistance of a glycobioinformatics tool, GlycoWorkBench (version 1.0.3353). (4) GC-MS linkage analysis was performed on partially methylated alditol acetates (PMAAs). (5) Sialidase S digestion was followed by manual assignment of the composition (numbers of Hex, Fuc, etc.) of the glycans derived from MALDI-TOF MS in positive ion mode. (6) Sialidase S digestion was followed by MALDI-TOF/TOF MS/MS analyses of the following ions: *m/z* 3143 and 4939. All MS/MS spectra were annotated manually with the assistance of a glycobioinformatics tool, GlycoWorkBench (version 1.0.3353). (7) The β1,4-galactosyltransferase reaction was followed by manual assignment of the composition (numbers of Hex, Fuc, etc.) of the glycans derived from MALDI-TOF MS in positive ion mode.

STB N-glycans—(1) All N-glycans were presumed to have a Manα1–6(Manα1–3)Manβ1–4GlcNAcβ1–4GlcNAc core structure based on knowledge of the N-glycan biosynthetic pathway and PNGase F specificity. (2) The composition (numbers of Hex, Fuc, etc.) of the glycans derived from MALDI-TOF MS in positive ion mode were manually interpreted. (3) MALDI-TOF/TOF MS/MS analyses were carried out on the following ions: *m/z* 2592, 2635, 2837, 2850, 3141, 3212, 3300, and 3416. All MS/MS spectra were annotated manually with the assistance of a glycobioinformatics tool, GlycoWorkBench (version 1.0.3353). (4) GC-MS linkage analysis was performed using partially methylated alditol acetates (PMAAs). (5) Sialidase S digestion was followed by manual assignment of the composition (numbers of Hex, Fuc, etc.) of the glycans derived from MALDI-TOF MS in positive ion mode. (6) Sialidase S digestion was followed by MALDI-TOF/TOF MS/MS analyses of following ions: *m/z* 3143 and 4939. All MS/MS spectra were annotated manually with the assistance of a glycobioinformatics tool, GlycoWorkBench (version 1.0.3353). The β1,4-galactosyltransferase reaction was followed by manual assignment of the composition (numbers of Hex, Fuc, etc.) of the glycans derived from MALDI-TOF MS in positive ion mode.

EVT N-glycans—(1) All N-glycans were presumed to have a Manα1–6(Manα1–3)Manβ1–4GlcNAcβ1–4GlcNAc core structure based on knowledge of the N-glycan biosynthetic pathway and PNGase F specificity. (2) The composition (numbers of Hex, Fuc, etc.) of the glycans derived from MALDI-TOF MS in positive ion mode were manually interpreted. (3) MALDI-TOF/TOF MS/MS analyses were carried out on the following ions: *m/z* 2519, 2850, 3141, 3212, 3415, 3964, and 4041. All MS/MS spectra were annotated manually with the assistance of a glycobioinformatics tool, GlycoWorkBench (version 1.0.3353). (4) Sialidase S digestion was followed by manual assignment of the composition (numbers of Hex, Fuc, etc.) of the glycans derived from MALDI-TOF MS in positive ion mode. (5) Sialidase S digestion was followed by MALDI-TOF/TOF MS/MS analyses of following ions: *m/z* 2489, 2519, 2693, 2968, 3142, 3387, 4040, and 4489. All MS/MS spectra were annotated manually with the assistance of a glycobioinformatics tool, GlycoWorkBench (version 1.0.3353) (26).

The symbolic nomenclature used in the all the spectra annotations (CTB, STB and EVT) is the same as the one used by the Consortium for Functional Glycomics (CFG) (http://www.functionalglycomics.org/) and the *Essentials for Glycobiology* on-line textbook (http://www.ncbi.nlm.nih.gov/books/NBK1931/figure/ch1.f5/?report=objectonl).

RESULTS

Analysis of N-glycans Associated with CTB—A modification of the Kliman procedure was employed to isolate samples of CTB from eight term placentas (22, 27). Each sample was subjected to glycomic profiling exactly as described in a previous study (16). High quality MALDI data were obtained for the N-glycans of all the CTB samples. There were no apparent differences in the spectra between eight individuals. A representative MALDI spectrum of N-glycans derived from CTB from one patient is shown in Fig. 1. The theoretical and observed m/z values of the glycans and the manual interpretation of the composition of these glycans are shown in supplemental Table S1. Signals for high mannose type N-glycans ($Man_{5-9}GlcNAc_2$) were abundant at *m/z* 1579.8, 1783.9, 1988.0, 2192.1, and 2396.1. In addition numerous signals for complex-type biantennary, triantennary and tetraantennary N-glycans were observed, and their structures are shown in the cartoon annotations in Fig. 1. To decrease the complexity of all the MALDI spectrum figures, the cartoon annotations for minor signals less than *m/z* 3250 are shown in supplemental Table S2. Nearly all the complex-type glycans carry core α1–6 linked fucose, consistent with their localization to the plasma membrane, and sialic acid is the major capping sugar on their N-acetyllactosamine antennae. The most abundant complex-type structures give signals at *m/z* 2431.1 (mono-sialylated biantennary), 2489.2 (non-sialylated, core fucosylated biantennary), 2850.3 (mono-sialylated, core fucosylated biantennary), 2966.3 (disialylated, core fucosylated biantennary), and 3211.4 (disialylated, core fucosylated biantennary). Interestingly three of these glycans have masses consistent with biantennary bisected type (BBSCT) structures (*m/z* 2489.2, 2850.3, and 3211.4). Minor signals for N-glycans bearing Lewis^x (*m/z* 2592.2, 2837.3, 3024.3) and sialyl-Lewis^x type antenna (*m/z* 3140.3) were also detected. Evidence for N-glycans bearing polylactosamine type sequences was indicated by the signal at *m/z* 3299.5.

Additional experiments were performed to firmly establish the glycan assignments shown in Fig. 1. First, to confirm assignments of BBSCT glycans, the N-glycan mixture was incubated with a β-galactosyltransferase in the presence of UDP-Gal. This enzymatic modification adds galactose to all antennae bearing terminal GlcNAc except for the bisecting GlcNAc which is sterically inaccessible to the enzyme. After this treatment, there was no detectable addition of galactose

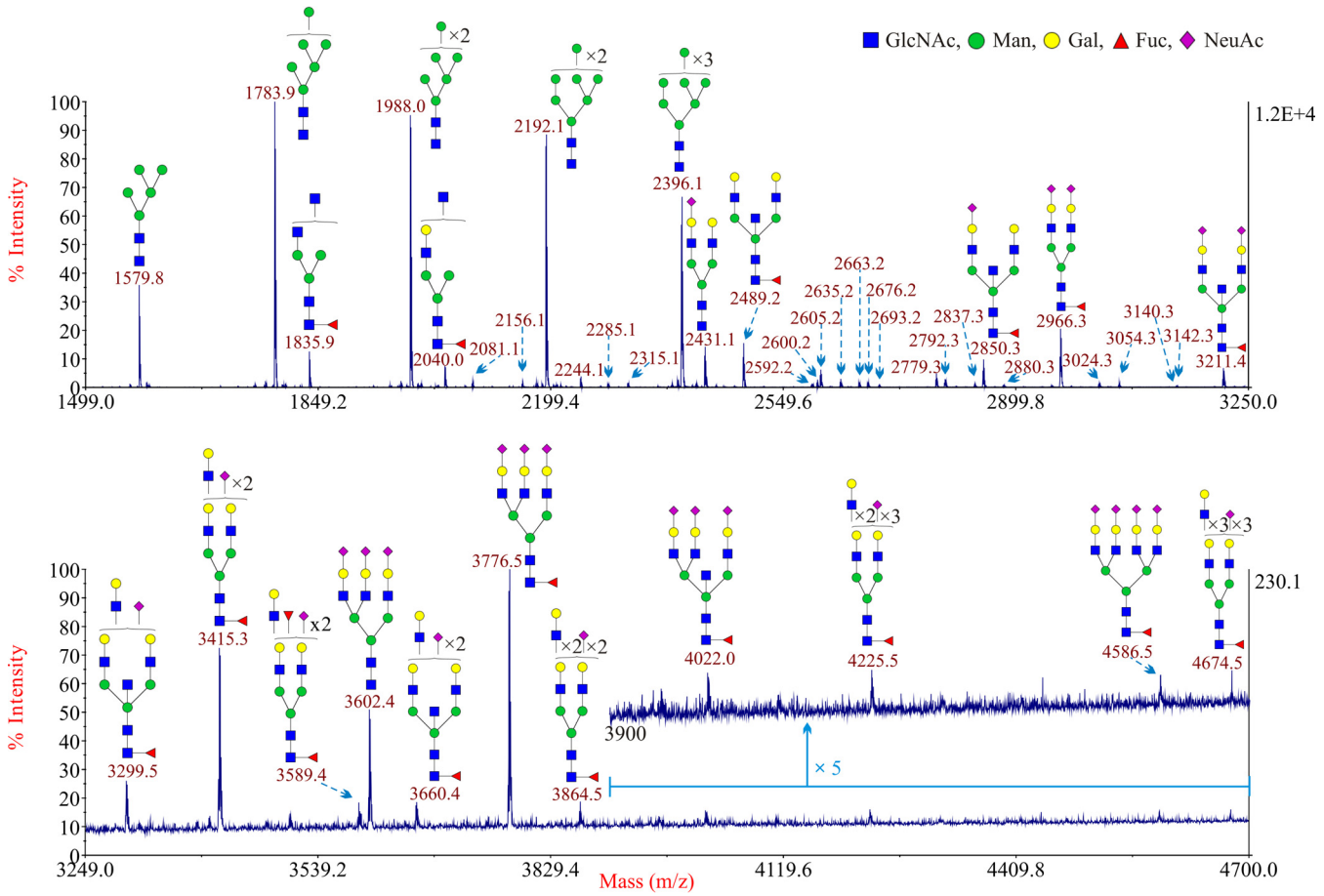

FIG. 1. **Annotated MALDI-TOF MS spectra of permethylated N-glycans from CTB.** The top panel shows the glycans in the mass range from 1499 to 3250 and the bottom panel shows the glycans in the mass range from 3249 to 4700. In the top panel, minor peaks are only labeled with their m/z values; their putative structures can be found in supplemental Table S2. Compared with the top panel, the bottom panel has been magnified ~53 times. Because of the fact that the peak signal in the mass range from 3900 to 4700 in the bottom panel is very weak, this part has been further magnified 5 times (upper trace). Profiles were obtained from the 50% acetonitrile fraction from a C18 Sep-Pak column. All ions are [M+Na]+. Putative structures are based on the molecular weight, N-glycan biosynthetic pathway, MS/MS data and enzymatic digestion results. Glycans at *m/z* 2966, 3777, and 4587 are clearly annotated, which is because of the fact that their structures are unequivocal because each antenna is capped with a sialic acid and thus they are homogeneous bi-, tri-, and tetraantennary glycans. However, the glycan structure is not always as unequivocal as the glycan at *m/z* 2966 as biosynthetically non-fully sialylated glycan molecular ion species could be made up of mixtures of structural isoforms. Annotations are simplified to biantennary structures, with additional LacNAc units and capping sugars listed outside the bracket, for mixtures of isobaric multiantennary glycans, some of which have antennae containing extended LacNAc repeats.

to putative BBSCT glycans (supplemental Fig. S1). In contrast, the truncated antennae of immature glycans (for example *m/z* 1835.9) were extended by galactose, confirming that the β-galactosyltransferase was reacting successfully. In addition, GC-MS linkage analysis of the glycan mixture (supplemental Table S3) provided further evidence for the presence of bisecting GlcNAc. The presence of Lewis^x and sialyl-Lewis^x type antenna on these N-glycans was confirmed by MS/MS analysis (supplemental Figs. S2, S3, S4). The glycan mixture was also treated with sialidase S, a bacterial neuraminidase that specifically hydrolyzes α2–3 linked sialic acid. MS analysis of the products indicated that the majority of the sialic acid was eliminated by this digestion. Substantial amounts of sialic acid were released, but signals for sialylated N-glycans remained at *m/z* 2431.2, 2676.3, 2880.3, and 3241.4, indicating that they were likely terminated with α2–6 linked sialic acid.

The N-glycans associated with CTB were treated with a neuraminidase (sialidase S) that specifically removes terminal α2–3 linked sialic acid. This enzymatic step removed nearly all of the sialic acid from these glycans, confirming that only a minor amount of sialic acid was α2–6 linked on glycoproteins associated with this cell type (Fig. 2). The major N-glycans that were detected after digestion were high mannose type N-glycans and the BBSCT N-glycan. This desialylation step also revealed minor amounts of N-glycans bearing polylactosamine sequences at *m/z* 3591.6, 3765.6, 3836.6, 4040.6, 4214.8, 4489.6, and 4938.6 (Fig. 2). MS/MS analysis of the peak at *m/z* 4938.6 (4939) showed that the maximum number of the LacNAc unit observed is five (supplemental Fig. S5).

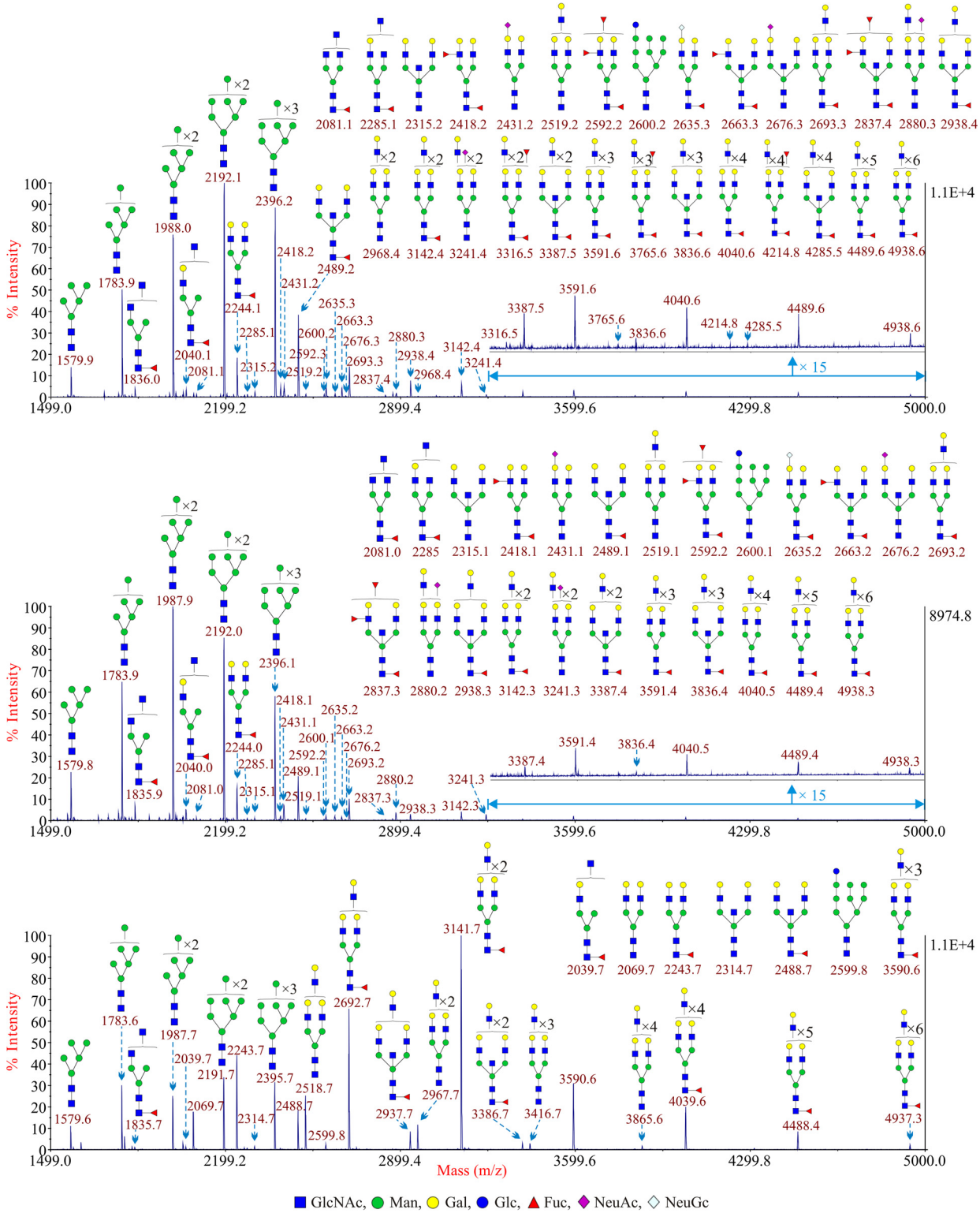

FIG. 2. **Annotated MALDI-TOF MS spectra of permethylated sialidase S treated N-glycans from CTB (upper panel), STB (middle panel) and EVT (lower panel).** Profiles were obtained from the 50% acetonitrile fraction from a C18 Sep-Pak column. All ions are $[M+Na]^+$. Putative structures are based on the molecular weight, N-glycan biosynthetic pathway, MS/MS data and enzymatic digestion results. Annotations are simplified to biantennary structures, with additional LacNAc units and capping sugars listed outside the bracket, for mixtures of isobaric multiantennary glycans, some of which have antennae containing extended LacNAc repeats. Minor peaks are only labeled with their *m/z* values; their putative structures can be found in supplemental Table S2.

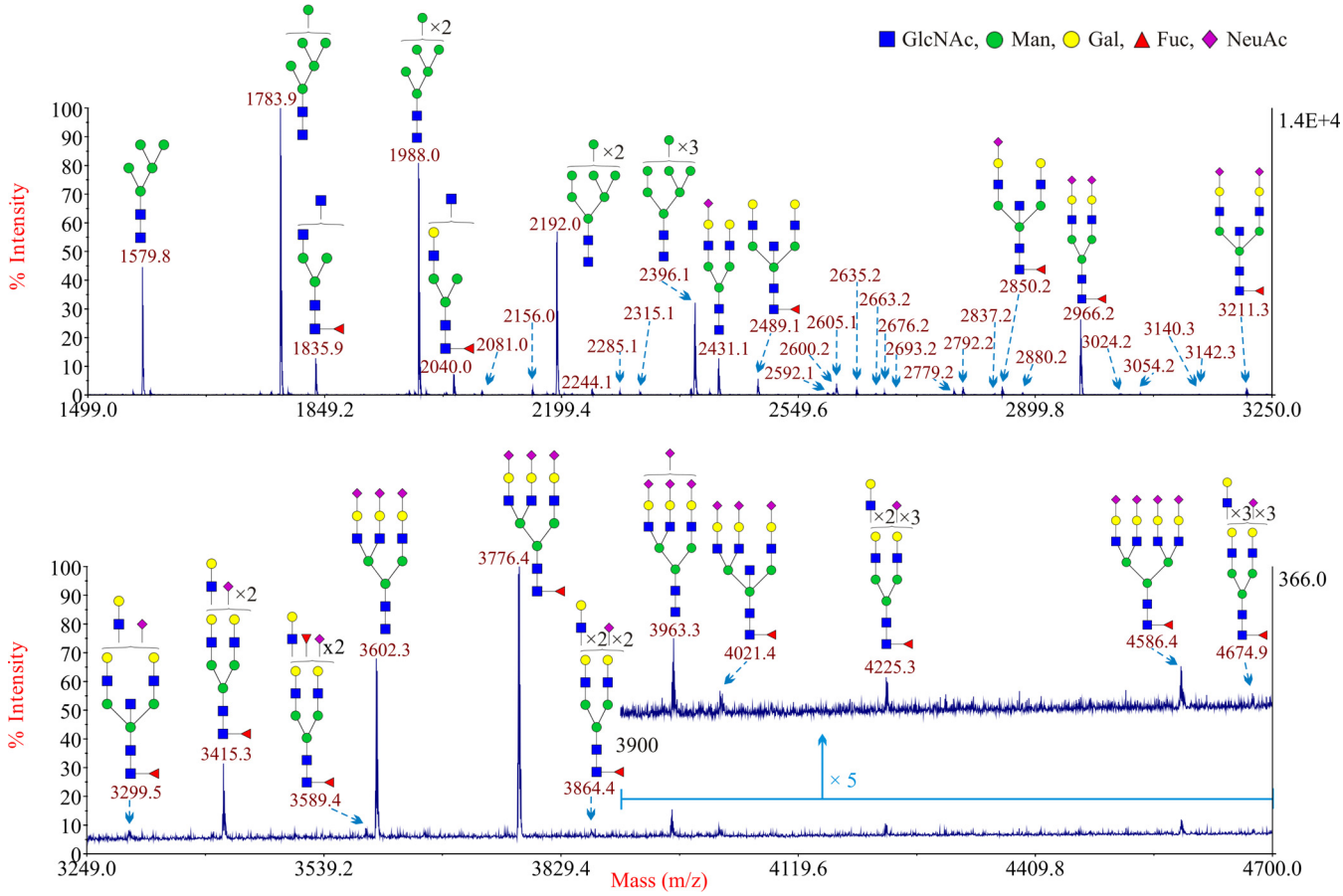

FIG. 3. **Annotated MALDI-TOF MS spectra of permethylated N-glycans from STB86.** The top panel shows the glycans in the mass range from 1499 to 3250 and the bottom panel shows the glycans in the mass range from 3249 to 4700. In the top panel, minor peaks are only labeled with their *m/z* values; their putative structures can be found in supplemental Table S2. Compared with the top panel, the bottom panel has been magnified ~37 times. Because of the fact that the peak signal in the mass range from 3900 to 4700 in the bottom panel is weaker, this part has been further magnified five times (upper trace). Profiles were obtained from the 50% acetonitrile fraction from a C18 Sep-Pak column. All ions are [M+Na]+. Putative structures are based on the molecular weight, N-glycan biosynthetic pathway, MS/MS data and enzymatic digestion results. Glycans at m/z 2966, 3777, and 4587 are clearly annotated, which is because of the fact that their structures are unequivocal because each antenna is capped with a sialic acid and thus they are homogeneous bi-, tri-, and tetraantennary glycans. However, the glycan structure is not always as unequivocal as the glycan at *m/z* 2966 as biosynthetically non-fully sialylated glycan molecular ion species could be made up of mixtures of structural isoforms. Annotations are simplified to biantennary structures, with additional LacNAc units and capping sugars listed outside the bracket, for mixtures of isobaric multiantennary glycans, some of which have antennae containing extended LacNAc repeats.

Glycomic Analysis of Human STB—These trophoblasts were obtained after *in vitro* differentiation of primary CTB as described previously (22, 27). They were subjected to the same procedure that was employed to analyze the CTB N-glycome (16). The theoretical and observed m/z values of the glycans and the manual interpretations of the composition of these glycans are shown in supplemental Table S4. There were no apparent differences in the spectra between individuals. A representative MALDI spectrum is shown in Fig. 3. There were essentially no differences in glycan expression between STB and CTB. This same overlap was also observed after sialidase S digestion of N-glycans derived from STB (Fig. 2). The major signals were for the high mannose type N-glycans ($Man_{5-9}GlcNAc_2$) and the BBSCT N-glycan (*m/z* 2489.1).

Glycomic Analysis of Human EVT—This subpopulation of trophoblasts was subjected to glycomic analysis to determine if there were any differences between them and other types of trophoblasts. The theoretical and observed *m/z* values of the glycans and the manual interpretations of the composition of these glycans are shown in supplemental Table S5. Although the N-glycans linked to EVT were very similar to those associated with CTB and STB, there were major differences in levels of expression (Fig. 4). The larger complex-type N-glycans were far more prevalent in EVT, which can be most readily observed via the comparison of glycans after sialidase S digestion (Fig. 2). The most abundant peak, after the removal of α2–3 linked sialic acid, was *m/z* 3141.7, which corresponds to a complex type N-glycan with four LacNAc units in its antennae. This peak was accompanied by a prominent

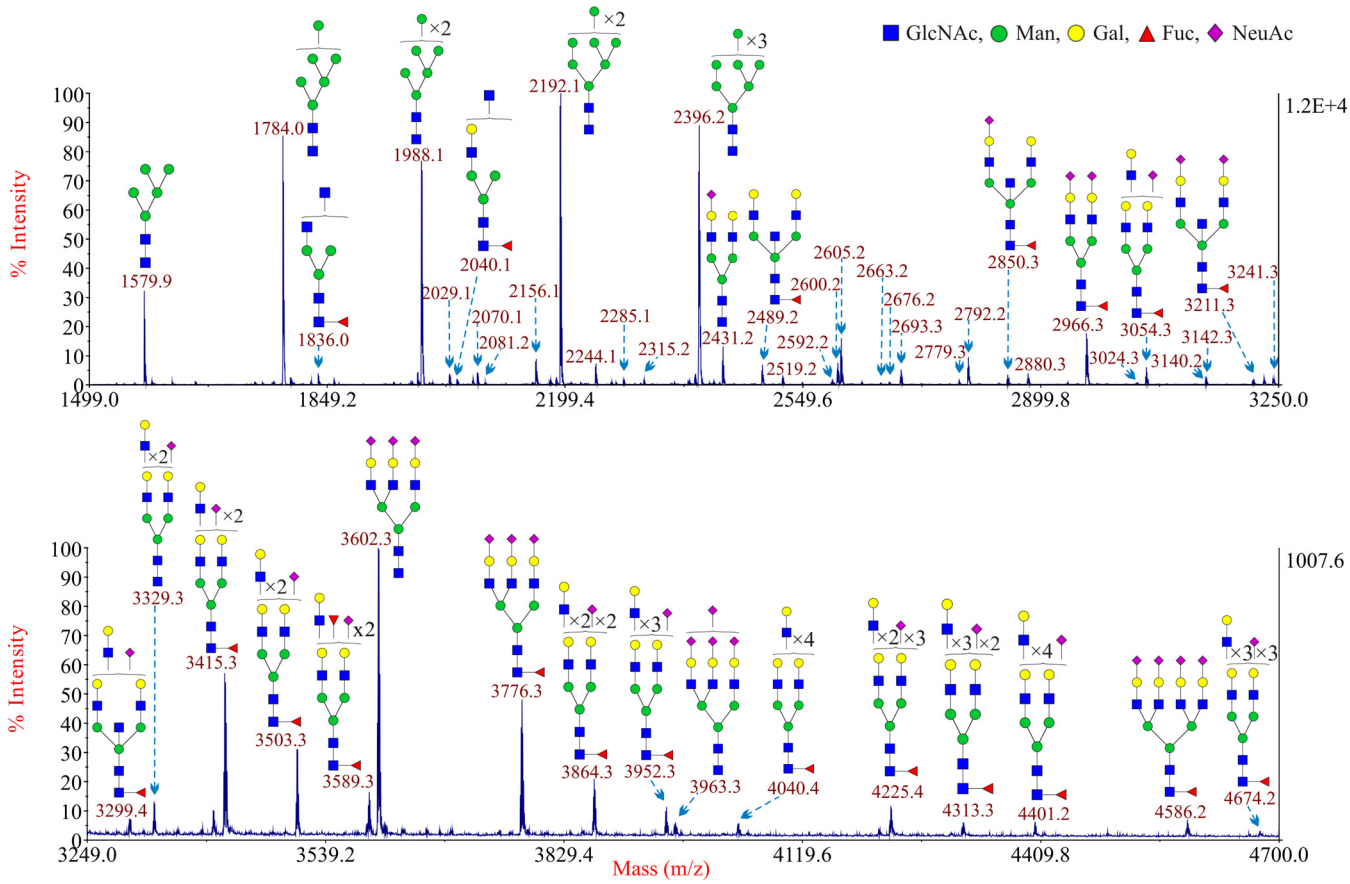

FIG. 4. **Annotated MALDI-TOF MS spectra of permethylated N-glycans from EVT.** The top panel shows the glycans in the mass range from 1499 to 3250 and the bottom panel shows the glycans in the mass range from 3249 to 4700. Minor peaks are only labeled with their *m/z* values; their putative structures can be found in supplemental Table S2. Compared with the top panel, the bottom panel has been magnified ~12 times. Profiles were obtained from the 50% acetonitrile fraction from a C18 Sep-Pak column. All ions are [M+Na]+. Putative structures are based on the molecular weight, N-glycan biosynthetic pathway, MS/MS data and enzymatic digestion results. Glycans at *m/z* 2966, 3777, and 4587 are clearly annotated, which is because of the fact that their structures are unequivocal because each antenna is capped with a sialic acid and thus they are homogeneous bi-, tri-, and tetraantennary glycans. However, the glycan structure is not always as unequivocal as the glycan at *m/z* 2966 as biosynthetically non-fully sialylated glycan molecular ion species could be made up of mixtures of structural isoforms. Annotations are simplified to biantennary structures, with additional LacNAc units and capping sugars listed outside the bracket, for mixtures of isobaric multiantennary glycans, some of which have antennae containing extended LacNAc repeats.

series of N-glycans with extended polylactosamine antennae containing additional LacNAc moieties (*m/z* 3590.6, 4039.6, 4488.4, and 4937.3). These glycans were far more abundant in EVT than in either CTB or STB. As a consequence, the relative abundance of the BBSCT N-glycan approximately *m/z* 2489 became less prominent in the overall spectrum of EVT compared with the other complex N-glycans. Another important difference was the absence of any detectable sialylated glycans after digestion with sialidase S. This result confirmed that all of the sialic acid associated with EVT is attached via α2–3 linkages.

DISCUSSION

The N-glycans associated with different types of human trophoblasts were analyzed in this study. A specific caveat to this analysis is that the STB were differentiated from CTB *in vitro* (22, 27). However, the microvillous membrane of human STB derived from the placenta stain intensely with lectins that bind to: (1) high mannose type N-glycans (Concanavalin A); (2) biantennary bisecting type N-glycans (erythroagglutinating phytohemagglutinin); (3) N-glycans bearing a core α1–6 linked fucose (*Pisum sativum* agglutinin); and (4) terminal α2–3 linked sialic acid (*Maackia amurensis* agglutinin) (28). By contrast, these microvillous membranes stain very poorly with a lectin that specifically binds to α2–6 linked sialic acid (*Sambucus nigra* agglutinin) (28). These lectin binding results are consistent with the glycomic analysis of STB presented in this report.

The human placenta nourishes the fetus during its development. This organ also negotiates the peaceful co-existence of the mother and her histoincompatible fetus during pregnancy. Specific adaptations have been made that enable 85–90% of women to fully accommodate their fetus until development *in utero* is complete. Trophoblasts are placental

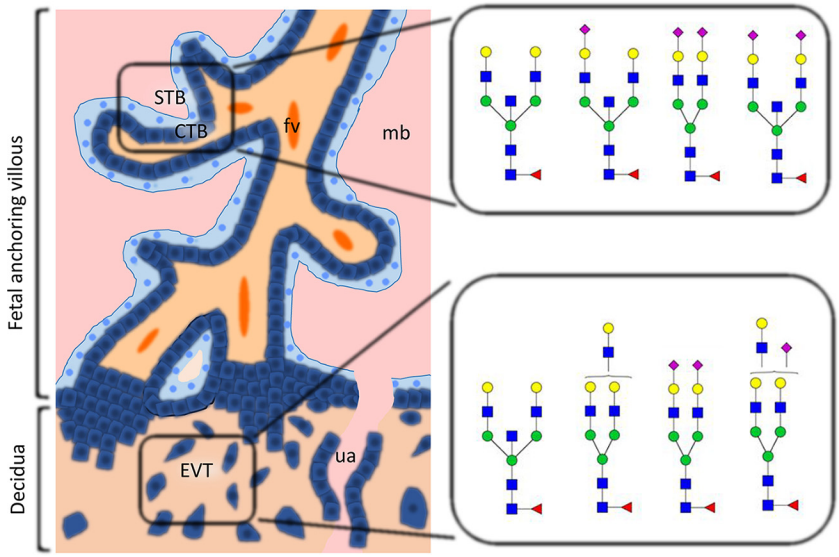

FIG. 5. **Differential glycosylation pattern expression on human trophoblast.** This figure summarizes the types of glycans that are characteristic of the cytotrophoblast (CTB), syncytiotrophoblast (STB), and extravillous cytotrophoblast (EVT). All three cell types express abundant high mannose glycans in addition to complex glycans. BBSCT N-glycans are found in all cell types, but are more abundant in CTB and STB than in EVT. EVT cells displayed higher levels of multiantennary and polylactosamine type N-glycans than CTB and STB. Abbreviations: fetal vessel (fv); maternal blood; uterine artery (ua). ■ GlcNAc ● Man ● Gal ▲ Fuc ♦ NeuAc.

cells that encounter maternal immune cells at two distinct interfaces. STB and CTB interact with maternal immune cells at the villous interface. EVT and their derivatives come into direct physical contact with maternal immune cells during their invasion of the decidua, myometrium and spiral arteries. The current study was undertaken to determine if functional glycosylation of trophoblasts could contribute to accommodation of the histoincompatible human fetus.

Glycosylation of Villous Trophoblasts—Our glycomic analyses of CTB and STB reveal that these cells express both high mannose and complex-type glycans. The majority of the latter are core fucosylated, biantennary structures with LacNAc or oligo-LacNAc antennae that are partially capped with α2–3 linked (major) or α2–6 linked (minor) sialic acid. A tiny portion of the glycome carries fucosylated antennae in Lewis$^{x/y}$ and sialyl-Lewis^{x}-type sequences. Significantly, many of the biantennary glycans have a bisecting GlcNAc. These N-glycans have previously been implicated in the suppression of NK cell cytotoxicity in highly specialized assay systems (29, 30). STB and CTB are highly resistant to NK cell-mediated cytotoxicity *in vitro* (10, 11). Whether or not this elevated expression of biantennary bisecting type N-glycans on STB and CTB plays a role in protecting these HLA class I negative cell types from NK cell mediated cytotoxicity is a topic for further investigation.

Expression of Glycans on EVT—Notably, the profile of N-glycans in EVT was different from those observed in villous trophoblasts, with EVT expressing relatively lower levels of biantennary bisecting type N-glycans and much higher levels of triantennary and tetraantennary N-glycans. N-glycans decorated with polylactosamine sequences were also considerably elevated in EVT compared with either CTB or STB. Unlike these villous trophoblasts, the sialylated N-glycans associated with EVT were also exclusively capped with α2–3 linked NeuAc. Our finding of the expression of polylactosamine-decorated N-glycans in EVT support previous findings by Fisher and coworkers. These investigators demonstrated that HLA-G produced by EVT and secreted into amniotic fluid migrates as a polydisperse band between 35–50 kDa that is collapsed into a single 35–36 kDa band after digestion with endo-β-galactosidase, an enzyme that specifically depolymerizes polylactosamine sequences (31, 32). Together, these findings suggest that a substantial proportion of native HLA-G molecules in EVT are decorated with polylactosamine sequences.

The expression of bisecting type N-glycans, though lower than in STB or CTB, could nonetheless provide EVT with some measure of protection from dNK cell responses. However, the exact level of protection remains a matter of conjecture with the available data. Results from one study suggest that dNK cells are incapable of forming mature activating synapses with EVT and thus are not cytotoxic (33). Other groups have reported that EVT are susceptible to lysis by dNK cells (12–14). Fisher and coworkers have provided evidence that decidual macrophages induce tolerance to EVT via their secretion of transforming growth factor-β1 (12). These observations are complicated by the presence of glycodelin-A and CA125, two soluble factors that are produced in abundance in the endometrium and decidua from the initiation of implantation up until the 20th week of gestation. Glycodelin-A and CA125 also suppress NK cell cytotoxicity *in vitro* (34–38). NK cell cytotoxicity is also directly suppressed by galectin-3 that is also present at elevated levels in the uterus during pregnancy (39, 40). These findings suggest that there are likely redundant pathways for the induction of NK cell tolerance in the endometrium and decidua during the first two trimesters of human pregnancy.

Expression of Galectins (LGALS) and Galectin Ligands in the Pregnant Uterus—Galectins are a family of β-galactoside binding proteins that express one or two conserved carbohy-

drate recognition domains (40–42). Elevated expression of GALS-1, -3, -8, -9, -13, -14, and -16 has been documented in the placenta and the endometrium/decidua during human pregnancy (40). Galectins act as both extracellular and intracellular modulators of diverse biological activities including trophoblast migration and invasion, syncytium formation, and immune modulation (41–45).

Several groups have tested the carbohydrate binding specificities of galectins via a variety of different methods (46–49). Considerable data have been obtained by analyzing the binding of galectins to different versions of the glycan array available on the public Consortium for Functional Glycomics (CFG) web site (http://www.functionalglycomics.org). Galectins are characterized by a near universal affinity for lacNAc (Galβ1–4GlcNAc). Many can accommodate substitution of the terminal β-linked Gal at the 3 but not the 6 position (46–49). This specificity confirms that galectins can bind to terminal NeuAcα2–3Galβ1–4GlcNAc sequences, but not to those capped with NeuAcα2–6Galβ1–4GlcNAc sequences (46). Nearly all of the sialic acid associated with STB and CTB was determined to be α2–3 linked in the current analyses. Only α2–3 linked sialic acid was detectable in the N-glycans derived from EVT. Galectins also display higher affinity for triantennary and tetraantennary N-glycans terminated with LacNAc sequences than for biantennary N-glycans of the same type (46–49). Galectin-3, -8, and -9 present in the uterus preferentially exhibit higher affinity for polylactosamine sequences (46). Glycomic analyses performed in this study indicate that EVT express a higher level of polylactosamine sequences and tri- and tetraantennary N-glycans. Galectin-1 binds to the biantennary bisecting type N-glycan based on glycan array data available at the CFG website. This specificity is consistent with the binding of galectin-1 to the surface of CTB that was reported in a previous study (50). Analysis of galectin binding to STB, CTB and EVT could be useful in the future for defining the immune modulatory effects of these carbohydrate binding proteins in the female urogenital tract.

In summary, in this study we have performed glycomic analysis of CTB, STB and EVT. We observed complex N-glycosylation on all of these cell types. The results of this study suggest the possibility that maternal-fetal tolerance could be influenced by the differential glycosylation of human trophoblasts populations. Whether aberrant glycosylation could contribute to inappropriate maternal-fetal immune response and poor pregnancy outcomes is certainly an issue for further investigation. Testing of these hypotheses will involve the analysis of glycosylation in trophoblasts in normal and complicated pregnancies, characterization of glycosylation changes in trophoblasts during development, and immunological analysis of any observed differences to determine their effects on maternal-fetal tolerance.

Acknowledgments—We thank P. Moschansky and Christine Wuillemin for their excellent technical assistance in generating this work.

* This study was supported by: the Life Sciences Mission Enhancement Reproductive Biology Program funded by the State of Missouri (to G.F.C.); Grants BB/K016164/1 and BB/F008309/1 from the Biotechnology and Biological Sciences Research Council (to A.D. and S.M.H.); Deutsche Forschungsgemeinschaft (DFG) grant BL1115/2–1 and Charite UFF 2015–710 (to S.M.B.); and the Swiss National Science Foundation grant 31003A-127392 (to M.C.). A.D. is a Wellcome Trust Senior Research Investigator.

S This article contains supplemental material.

¶¶ To whom correspondence should be addressed: Obstetrics, Gynecology and Women's Health, University of Missouri, 1 Hospital Drive HSC M658, Columbia, MO 65211. Tel.: 1 (573) 882-1725; Fax: 882-9010; E-mail: clarkgf@health.missouri.edu; Department of Life Sciences, Faculty of Natural Sciences, Imperial College London, South Kensington Campus, London SW7 2AZ, UK. Tel: +44-207-594-5219; E-mail: a.dell@imperial.ac.uk; Division of General Internal and Psychosomatic Medicine, Reproductive Medicine Research Group, Charité Center for Internal Medicine and Dermatology, Charité-Universitätsmedizin Berlin, Berlin, Germany. Tel: +49 30 450 553791; Fax: +49 30 450 553946; E-mail: Sandra.Blois@charite.de.

REFERENCES

1. Longtine, M. S., Chen, B., Odibo, A. O., Zhong, Y., and Nelson, D. M. (2012) Caspase-mediated apoptosis of trophoblasts in term human placental villi is restricted to cytotrophoblasts and absent from the multinucleated syncytiotrophoblast. *Reproduction* **143,** 107–121
2. Brownbill, P., Mahendran, D., Owen, D., Swanson, P., Thornburg, K. L., Nelson, D. M., and Sibley, C. P. (2000) Denudations as paracellular routes for a-fetoprotein and creatinine across the human syncytiotrophoblast. *Am. J. Physiol. Regul. Integr. Comp. Physio.l* **278,** R677–R683
3. Handwerger, S. (2010) New insights into the regulation of human cytotrophoblast cell differentiation. *Mol. Cell. Endocrinol.* **323,** 94–104
4. Robson, A., Harris, L. K., Innes, B. A., Lash, G. E., Aljunaidy, M. M., Aplin, J. D., Baker, P. N., Robson, S. C., and Bulmer, J. N. (2012) Uterine natural killer cells initiate spiral artery remodeling in human pregnancy. *FASEB J.* **26,** 4876–4885
5. Thaler, I., Manor, D., Itskovitz, J., Rottem, S., Levit, N., Timor-Tritsch, I., and Brandes, J. M. (1990) Changes in uterine blood flow during human pregnancy. *Am. J. Obstet. Gynecol.* **162,** 121–125
6. Kliman, H. J. (2000) Uteroplacental blood flow. The story of decidualization, menstruation, and trophoblast invasion. *Am. J. Pathol.* **157,** 1759–1768
7. Juch, H., Blaschitz, A., Dohr, G., and Hutter, H. (2012) HLA class I expression in the human placenta. *Wien. Med. Wochenschr.* **162,** 196–200
8. Hutter, H., Hammer, A., Blaschitz, A., Hartmann, M., Ebbesen, P., Dohr, G., Ziegler, A., and Uchanska-Ziegler, B. (1996) Expression of HLA class I molecules in human first trimester and term placenta trophoblast. *Cell Tissue Res.* **286,** 439–447
9. Ljunggren, H. G., and Karre, K. (1990) In search of the 'missing self': MHC molecules and NK cell recognition. *Immunol. Today* **11,** 237–244
10. King, A., Birkby, C., and Loke, Y. W. (1989) Early human decidual cells exhibit NK activity against the K562 cell line but not against first trimester trophoblast. *Cell. Immunol.* **118,** 337–344
11. King, A., and Loke, Y. W. (1990) Human trophoblast and JEG choriocarcinoma cells are sensitive to lysis by IL-2-stimulated decidual NK cells. *Cell. Immunol.* **129,** 435–448
12. Co, E. C., Gormley, M., Kapidzic, M., Rosen, D. B., Scott, M. A., Stolp, H. A., McMaster, M., Lanier, L. L., Barcena, A., and Fisher, S. J. (2013) Maternal decidual macrophages inhibit NK cell killing of invasive cytotrophoblasts during human pregnancy. *Biol. Reprod.* **88,** 155
13. Nakashima, A., Shiozaki, A., Myojo, S., Ito, M., Tatematsu, M., Sakai, M., Takamori, Y., Ogawa, K., Nagata, K., and Saito, S. (2008) Granulysin produced by uterine natural killer cells induces apoptosis of extravillous trophoblasts in spontaneous abortion. *Am. J. Pathol.* **173,** 653–664
14. Jones, R. K., Bulmer, J. N., and Searle, R. F. (1997) Cytotoxic activity of endometrial granulated lymphocytes during the menstrual cycle in humans. *Biol. Reprod.* **57,** 1217–1222
15. Whitley, G. S., and Cartwright, J. E. (2009) Trophoblast-mediated spiral artery remodelling: a role for apoptosis. *J. Anat.* **215,** 21–26
16. Pang, P. C., Chiu, P. C., Lee, C. L., Chang, L. Y., Panico, M., Morris, H. R.,

Haslam, S. M., Khoo, K. H., Clark, G. F., Yeung, W. S., and Dell, A. (2011) Human sperm binding is mediated by the sialyl-Lewis^x oligosaccharide on the zona pellucida. *Science* **333,** 1761–1764
17. Easton, R. L., Patankar, M. S., Clark, G. F., Morris, H. R., and Dell, A. (2000) Pregnancy-associated changes in the glycosylation of Tamm-Horsfall glycoprotein. Expression of sialyl Lewis^x sequence on core 2 type O-glycans derived from uromodulin. *J. Biol. Chem.* **275,** 21928–21938
18. Chui, D., Sellakumar, G., Green, R., Sutton-Smith, M., McQuistan, T., Marek, K., Morris, H., Dell, A., and Marth, J. (2001) Genetic remodeling of protein glycosylation in vivo induces autoimmune disease. *Proc. Natl. Acad. Sci. U.S.A.* **98,** 1142–1147
19. Jia, N., Barclay, W. S., Roberts, K., Yen, H. L., Chan, R. W., Lam, A. K., Air, G., Peiris, J. S., Dell, A., Nicholls, J. M., and Haslam, S. M. (2014) Glycomic characterization of respiratory tract tissues of ferrets: implications for its use in influenza virus infection studies. *J. Biol. Chem.* **289,** 28489–28504
20. Dell, A., Morris, H. R., Easton, R. L., Panico, M., Patankar, M., Oehniger, S., Koistinen, R., Koistinen, H., Seppala, M., and Clark, G. F. (1995) Structural analysis of the oligosaccharides derived from glycodelin, a human glycoprotein with potent immunosuppressive and contraceptive activities. *J. Biol. Chem.* **270,** 24116–24126
21. Kui Wong, N., Easton, R. L., Panico, M., Sutton-Smith, M., Morrison, J. C., Lattanzio, F. A., Morris, H. R., Clark, G. F., Dell, A., and Patankar, M. S. (2003) Characterization of the oligosaccharides associated with the human ovarian tumor marker CA125. *J. Biol. Chem.* **278,** 28619–28634
22. Kliman, H. J., Nestler, J. E., Sermasi, E., Sanger, J. M., and Strauss, J. F., 3rd (1986) Purification, characterization, and in vitro differentiation of cytotrophoblasts from human term placentae. *Endocrinology* **118,** 1567–1582
23. Bischof, P., Haenggeli, L., and Campana, A. (1995) Gelatinase and oncofetal fibronectin secretion is dependent on integrin expression on human cytotrophoblasts. *Hum. Reprod.* **10,** 734–742
24. Jang-Lee, J., North, S. J., Sutton-Smith, M., Goldberg, D., Panico, M., Morris, H., Haslam, S., and Dell, A. (2006) Glycomic profiling of cells and tissues by mass spectrometry: fingerprinting and sequencing methodologies. *Methods Enzymol.* **415,** 59–86
25. North, S. J., Jang-Lee, J., Harrison, R., Canis, K., Ismail, M. N., Trollope, A., Antonopoulos, A., Pang, P. C., Grassi, P., Al-Chalabi, S., Etienne, A. T., Dell, A., and Haslam, S. M. (2010) Mass spectrometric analysis of mutant mice. *Methods Enzymol.* **478,** 27–77
26. Ceroni, A., Maass, K., Geyer, H., Geyer, R., Dell, A., and Haslam, S. M. (2008) GlycoWorkbench: a tool for the computer-assisted annotation of mass spectra of glycans. *J. Proteome Res.* **7,** 1650–1659
27. Chen, B., Longtine, M. S., Sadovsky, Y., and Nelson, D. M. (2010) Hypoxia downregulates p53 but induces apoptosis and enhances expression of BAD in cultures of human syncytiotrophoblasts. *Am. J. Physiol. Cell Physiol* **299,** C968–C976
28. Jones, C. J., Carter, A. M., Aplin, J. D., and Enders, A. C. (2007) Glycosylation at the fetomaternal interface in hemomonochorial placentae from five widely separated species of mammal: is there evidence for convergent evolution? *Cells Tissues Organs* **185,** 269–284
29. el Ouagari, K., Teissie, J., and Benoist, H. (1995) Glycophorin A protects K562 cells from natural killer cell attack. Role of oligosaccharides. *J. Biol. Chem.* **270,** 26970–26975
30. Yoshimura, M., Ihara, Y., Ohnishi, A., Ijuhin, N., Nishiura, T., Kanakura, Y., Matsuzawa, Y., and Taniguchi, N. (1996) Bisecting N-acetylglucosamine on K562 cells suppresses natural killer cytotoxicity and promotes spleen colonization. *Cancer Res.* **56,** 412–418
31. McMaster, M., Zhou, Y., Shorter, S., Kapasi, K., Geraghty, D., Lim, K. H., and Fisher, S. (1998) HLA-G isoforms produced by placental cytotrophoblasts and found in amniotic fluid are due to unusual glycosylation. *J. Immunol.* **160,** 5922–5928
32. Fukuda, M. N., and Matsumura, G. (1976) Endo-β-galactosidase of Escherichia freundii. Purification and endoglycosidic action on keratan sulfates, oligosaccharides, and blood group active glycoprotein. *J. Biol. Chem.* **251,** 6218–6225
33. Kopcow, H. D., Allan, D. S., Chen, X., Rybalov, B., Andzelm, M. M., Ge, B., and Strominger, J. L. (2005) Human decidual NK cells form immature activating synapses and are not cytotoxic. *Proc. Natl. Acad. Sci. U.S.A.* **102,** 15563–15568
34. Okamoto, N., Uchida, A., Takakura, K., Kariya, Y., Kanzaki, H., Riittinen, L., Koistinen, R., Seppala, M., and Mori, T. (1991) Suppression by human placental protein 14 of natural killer cell activity. *Am. J. Reprod. Immunol.* **26,** 137–142
35. Belisle, J. A., Horibata, S., Jennifer, G. A., Petrie, S., Kapur, A., Andre, S., Gabius, H. J., Rancourt, C., Connor, J., Paulson, J. C., and Patankar, M. S. (2010) Identification of Siglec-9 as the receptor for MUC16 on human NK cells, B cells, and monocytes. *Mol. Cancer* **9,** 118
36. Patankar, M. S., Jing, Y., Morrison, J. C., Belisle, J. A., Lattanzio, F. A., Deng, Y., Wong, N. K., Morris, H. R., Dell, A., and Clark, G. F. (2005) Potent suppression of natural killer cell response mediated by the ovarian tumor marker CA125. *Gynecol. Oncol.* **99,** 704–713
37. Niloff, J. M., Knapp, R. C., Schaetzl, E., Reynolds, C., and Bast, R. C., Jr. (1984) CA125 antigen levels in obstetric and gynecologic patients. *Obstet. Gynecol.* **64,** 703–707
38. Julkunen, M., Rutanen, E. M., Koskimies, A., Ranta, T., Bohn, H., and Seppala, M. (1985) Distribution of placental protein 14 in tissues and body fluids during pregnancy. *Br. J. Obstet. Gynaecol.* **92,** 1145–1151
39. Wang, W., Guo, H., Geng, J., Zheng, X., Wei, H., Sun, R., and Tian, Z. (2014) Tumor-released galectin-3, a soluble inhibitory ligand of human NKp30, plays an important role in tumor escape from NK cell attack. *J. Biol. Chem.* **289,** 33311–33319
40. Blois, S. M., and Barrientos, G. (2014) Galectin signature in normal pregnancy and preeclampsia. *J. Reprod. Immunol.* 101- **102,** 127–134
41. Cummings, R. D., and Liu, F. T. (2009) Galectins. In: Varki, A., Cummings, R. D., Esko, J. D., Freeze, H. H., Stanley, P., Bertozzi, C. R., Hart, G. W., and Etzler, M. E., eds. *Essentials of Glycobiology*, 2010/03/20 Ed., Cold Spring Harbor Laboratory Press, Cold Spring Harbor
42. Than, N. G., Romero, R., Kim, C. J., McGowen, M. R., Papp, Z., and Wildman, D. E. (2012) Galectins: guardians of eutherian pregnancy at the maternal-fetal interface. *Trends Endocrinol. Metab.* **23,** 23–31
43. Bevan, B. H., Kilpatrick, D. C., Liston, W. A., Hirabayashi, J., and Kasai, K. (1994) Immunohistochemical localization of a β-D-galactoside-binding lectin at the human maternofetal interface. *Histochem. J.* **26,** 582–586
44. Fischer, I., Redel, S., Hofmann, S., Kuhn, C., Friese, K., Walzel, H., and Jeschke, U. (2010) Stimulation of syncytium formation in vitro in human trophoblast cells by galectin-1. *Placenta* **31,** 825–832
45. Kolundzic, N., Bojic-Trbojevic, Z., Kovacevic, T., Stefanoska, I., Kadoya, T., and Vicovac, L. (2011) Galectin-1 is part of human trophoblast invasion machinery–a functional study in vitro. *PloS One* **6,** e28514
46. Hirabayashi, J., Hashidate, T., Arata, Y., Nishi, N., Nakamura, T., Hirashima, M., Urashima, T., Oka, T., Futai, M., Muller, W. E., Yagi, F., and Kasai, K. (2002) Oligosaccharide specificity of galectins: a search by frontal affinity chromatography. *Biochim. Biophys. Acta* **1572,** 232–254
47. Hirabayashi, J., and Kasai, K. (1993) The family of metazoan metal-independent β-galactoside-binding lectins: structure, function and molecular evolution. *Glycobiology* **3,** 297–304
48. Brewer, C. F. (2004) Thermodynamic binding studies of galectin-1, -3 and -7. *Glycoconj. J.* **19,** 459–465
49. Gupta, D., Cho, M., Cummings, R. D., and Brewer, C. F. (1996) Thermodynamics of carbohydrate binding to galectin-1 from Chinese hamster ovary cells and two mutants. A comparison with four galactose-specific plant lectins. *Biochemistry* **35,** 15236–15243
50. Tirado-Gonzalez, I., Freitag, N., Barrientos, G., Shaikly, V., Nagaeva, O., Strand, M., Kjellberg, L., Klapp, B. F., Mincheva-Nilsson, L., Cohen, M., and Blois, S. M. (2013) Galectin-1 influences trophoblast immune evasion and emerges as a predictive factor for the outcome of pregnancy. *Mol. Hum. Reprod.* **19,** 43–53